The active catalytic species and its isomerisation in the catalytic carbonylation of methanol — a density functional study

ARTICLE *in* JOURNAL OF MOLECULAR STRUCTURE THEOCHEM · MAY 2001

Impact Factor: 1.37 · DOI: 10.1016/S0166-1280(00)00729-6

2 AUTHORS, INCLUDING:

Kari Laasonen
Aalto University
140 PUBLICATIONS **5,750** CITATIONS

SEE PROFILE

ELSEVIER

Journal of Molecular Structure (Theochem) 540 (2001) 91–100

THEO CHEM

www.elsevier.nl/locate/theochem

The active catalytic species and its isomerisation in the catalytic carbonylation of methanol — a density functional study

T. Kinnunen, K. Laasonen*

Department of Chemistry, University of Oulu, P.O. Box 3000, Oulu 90014, Finland

Received 30 June 2000; revised 10 July 2000; accepted 18 August 2000

Abstract

The Monsanto acetic acid process is one of the most effective ways to produce acetic acid industrially. This process has been studied experimentally but theoretical investigations are so far sparse. In the current work the active catalytic species $[Rh(CO)_2I_2]^-$ (**1**) and its isomerisation has been studied theoretically using the hybrid B3LYP exchange and correlation functional. Similar calculations has been performed for the iridium complex $[Ir(CO)_2I_2]^-$ (**2**) that also is catalytically active in the methanol carbonylation. Experimental work has confirmed the existence of the *cis* forms of the active catalytic species, but they do not rule out the possibility of the *trans* isomers. Our gas phase results show that *cis*-**1** has 4.95 kcal/mol lower free energy than *trans*-**1**, and *cis*-**2** has 10.39 kcal/mol lower free energy than *trans*-**2**. In the case of rhodium, *trans*-**1** can take part to the catalytic cycle but in case of iridium this is not very likely. We have also investigated the possible mechanisms of the *cis* to *trans* conversions. The ligand association mechanism gave free energy barrier of 13.7 kcal/mol for the rhodium complex and 19.8 kcal/mol for iridium. Thus the conversion for the rhodium complex is feasible whereas for iridium it is unlikely.

Keywords: Rhodium; Iridium; Density functional theory; Isomerisation; Carbonylation

1. Introduction

One of the most common ways to produce acetic acid industrially is the catalytic carbonylation of methanol by the Monsanto acetic acid process [1]. Although this method has been developed over 30 years ago it still retains the interest of the scientists. The Monsanto procedure is studied widely experimentally [1] but computational studies are sparse [2,3]. The active catalytic species in the process is a diiododicarbonylrhodate anion $[Rh(CO)_2I_2]^-$ (**1**) that is formed from various rhodium compounds and iodine promoters [4,5]. The active species undergoes the series of a standard organometallic reactions yielding acetic acid at low temperature and pressure. Proposed mechanism [4] for the Monsanto process is illustrated in Fig. 1.

At present we study the Monsanto process with ab initio calculations. With these techniques it is possible to examine the catalytic cycles step by step and get results that will give more insight to the processes. In the current paper we have concentrated on the active catalytic species $[Rh(CO)_2I_2]^-$ (**1**) and iridium complex $[Ir(CO)_2I_2]^-$ (**2**) that also is catalytically active in the methanol carbonylation [5,6]. In the iridium system, the catalysis cycle is very similar to that shown in Fig. 1. Experimental studies [1,4,6]

* Corresponding author. Tel.: +358-85-531-640; fax: +358-85-531-603.

E-mail addresses: tapani.kinnunen@oulu.fi (T. Kinnunen), kari.laasonen@oulu.fi (K. Laasonen).

0166-1280/01/$ - see front matter
PII: S0166-1280(00)00729-6

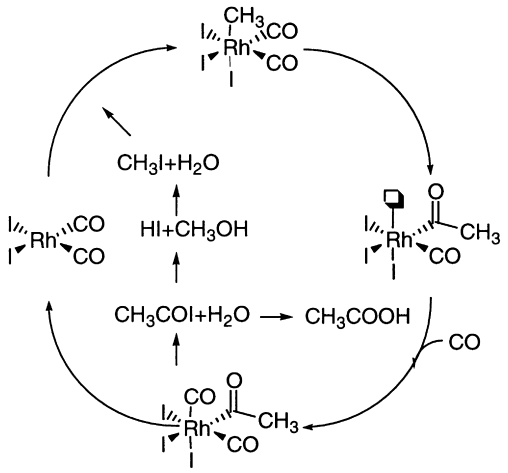

Fig. 1. Proposed mechanism of the Monsanto acetic acid process.

have confirmed the existence of *cis*-**1** and *cis*-**2** but *trans*-**1** and *trans*-**2** have not been observed. On the other hand the experiments do not rule out the *trans*-isomers. Our preliminary studies [7] show that the rate limiting step of the rhodium system, the methyl iodide addition to *trans*-**1** is easier than the addition to *cis*-**1** and therefore the reaction catalysed by *trans*-**1** can be a possible route in the Monsanto process. Overall the *trans* isomers of **1** and **2** are worth of studying. In addition we have studied the *cis–trans* isomerisation mechanism to see how large is the isomerisation barrier. In more general terms we believe that our calculations will also give some more understanding to the chemistry of the square-planar 16-electron d^8-complexes. Especially the isomerisation study is interesting because the topic has been studied very little computationally.

2. Computational details

Our calculations have been based on the hybrid B3LYP [8,9] exchange and correlation (XC) functional and we have used GAUSSIAN 98 [10] program package. The calculations have been performed with the SDD basis set. The SDD consists of a D95V for carbon, oxygen and hydrogen atoms. The Stuttgart/Dresden effective core potentials (ECP) with scalar relativistic corrections are used for rhodium, iridium and iodine. In addition, an extra fine integration grid has been applied. The B3LYP functional and SDD basis set has worked well in recent studies of organometallic catalysis systems [11,12]. We have also used some other XC-functionals and the results are qualitatively similar as will be reported here. Therefore

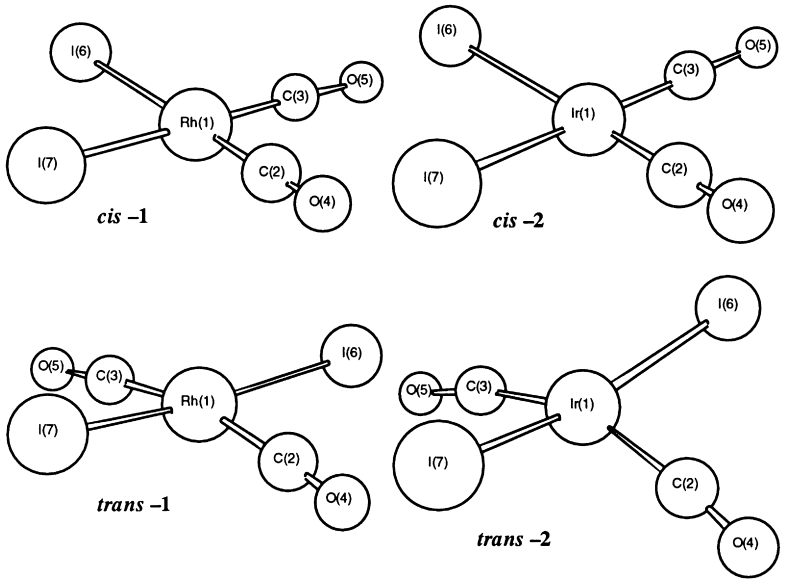

Fig. 2. The minimum energy structures of *cis*-**1**, *trans*-**1**, *cis*-**2** and *trans*-**2**. The *cis* structures are square planar while the *trans* are twisted.

Table 1
The bond lengths, angles and dihedral angle of *cis*-**1**, *trans*-**1**, *cis*-**2** and *trans*-**2**. M is the metal centre

	cis-**1**	*trans*-**1**	*cis*-**2**	*trans*-**2**
Distance (Å)				
M(1)–C(2)	1.853	1.905	1.853	1.897
C(2)–O(4)	1.185	1.179	1.188	1.187
M(1)–C(3)	1.853	1.905	1.853	1.897
C(3)–O(5)	1.185	1.179	1.188	1.187
M(1)–I(6)	2.759	2.741	2.778	2.755
M(1)–I(7)	2.759	2.741	2.778	2.755
Angle				
M(1)–C(2)–O(4)	178.2	175.9	178.6	170.6
M(1)–C(3)–O(5)	178.2	175.9	178.6	170.6
C(2)–M(1)–I(6)	179.8	90.3	178.9	91.6
C(2)–M(1)–I(7)	85.1	90.3	86.4	91.6
C(2)–M(1)–C(3)	95.1	165.7	94.7	151.1
I(6)–M(1)–I(7)	94.6	174.4	92.6	167.3
C(3)–M(1)–I(6)	85.1	90.3	86.4	91.6
C(3)–M(1)–I(7)	179.8	90.3	178.9	91.6
Dihedral angle				
I(7)–I(6)–M(1)–C(2)	180.0	97.1	180.0	75.6

we are confident that the computational scheme is adequate.

Minimum energy structures have been obtained with the Berny optimisation algorithm. The final structures of the transition states have been calculated with the GAUSSIAN 98 and the first guess for them has been determined with the synchronous transit-guided quasi-Newton methods (STQN). GAUSSIAN 98 has also been used to scan the potential energy surface (PES). The PES has been scanned with a constrained optimisation along a chosen reaction coordinate that has been a distance between two atoms. In addition, the frequencies have been calculated to verify the minimum energy and the transition state geometries. All the transition states have one imaginary frequency while the minimum energy structures have none. The free energies have been obtained by assuming rigid molecules and harmonic approximation to the vibrational states. Most of our studies have been performed in a gas phase and no symmetry constraints have been utilised. The PCM solvation model [13] has been used to investigate the *cis*–*trans* energy differences.

3. The active catalytic species $[Rh(CO)_2I_2]^-$ (1) and $[Ir(CO)_2I_2]^-$ (2)

We started by calculating the minimum energy structures for *cis*-**1**, *trans*-**1** and the corresponding iridium structures. The electronic structure of these 16-electron d^8-complexes were singlet. For *trans*-**1** the triplet state was 23 kcal/mol higher in energy. Singlet state is also consistent with the ligand field theory [14]. Fig. 2 illustrates the optimum geometries of the structures and Table 1 shows their bond lengths, angles and one dihedral angle.

The zero-point corrected potential energy difference between *cis*-**1** and *trans*-**1** is only 5.65 kcal/mol, the *cis* isomer being in the lower energy. Our result for the rhodium complexes is consistent with the experimental thermodynamics [15] for the square-planar complexes which indicate that generally the *cis* complexes are favoured by 5 kcal/mol. In the iridium analogues the zero-point corrected energy difference between *cis*-**2** and *trans*-**2** is 11.17 kcal/mol. The energy differences briefly reported by Cheong et al. [3] with BP86 XC-functional for the rhodium system is 8.20 kcal/mol and for iridium 16.00 kcal/mol. Our results are consistent with these. The free energy difference between *cis*-**1** and *trans*-**1** is 4.95 kcal/mol, approximated at 298.15 K. For **2**, the corresponding value is 10.39 kcal/mol. The calculated ΔG values are in agreement with the experimental thermodynamics that indicate the entropy effects generally favouring the *trans* isomers [15]. The relative stability of the *cis* complexes is partly due to the stronger internal bond energies which can be seen by comparing the minimum energy geometries of the *cis* and the *trans* isomers. The M–C bonds are shorter and therefore stronger in the *cis* isomers which is due to the more effective back bonding of the carbonyl ligands. Also in the *cis* form the C–O bonds are slightly longer (see Table 1). Overall, the calculated structures are consistent with other similar compounds but exact comparison cannot be made since we are not aware of any crystal structures for the active species.

Most of the structural data from the Monsanto process has been achieved via IR- or NMR-spectroscopy [1,4,6,16,17]. This data confirms only the *cis*-forms of **1** and **2** while the *trans* isomers have not been identified. In IR-spectroscopy, the validations have

Table 2
The calculated wave numbers and the ratio of the intensities of the CO-stretching modes for the catalysts **1** and **2**. $\nu_{(CO)sym}$ is the symmetric stretch and $\nu_{(CO)antisym}$ the antisymmetric stretch. Because the *trans* isomers are twisted, their symmetric CO-stretches are observed

Species	$\nu_{(CO)sym}$	$\nu_{(CO)antisym}$	$I_{\nu(CO)sym}/I_{\nu(CO)\ antisym}$
cis-**1**	1977.1	1911.8	1.174
trans-**1**	2000.4	1913.2	0.020
cis-**2**	1980.8	1910.2	1.015
trans-**2**	1974.9	1886.2	0.084

been made by measuring the wave numbers and the ratio of the intensities of the carbonyl stretching modes. The IR-spectrums [16] have two carbonyl stretches at wave numbers 2059 and 1988 cm^{-1} for **1** and 2046 and 1968 cm^{-1} for **2**. All these stretches have similar intensity. The high frequency bands correspond to symmetric CO-stretching modes and the low frequency bands to antisymmetric modes. In the case of the ideal square-planar complexes, according to the group theory, the experimental spectrums explain occurrence of the *cis* isomers. If two carbonyl ligands are in the exact *trans* position, the symmetric CO-stretch does not change the dipole moment and is IR inactive. So, in the ideal case the spectrum of the *trans* complex would have only one CO-stretching mode. However, this is not true because the *trans* forms of **1** and **2** have bended structures and one would expect to see two IR active CO-stretching modes in their spectra. We have calculated the frequencies for *cis*-**1**, *trans*-**1**, *cis*-**2** and *trans*-**2** and the results are shown in Table 2.

As expected both isomers of **1** and **2** posses two IR active modes. The spectrums of *cis*-**1** and *cis*-**2** agree quite well with the experimental ones while the spectrums of the *trans* isomers have the symmetric stretches with low intensities. Even both forms of **1** and **2** could exist the transform would have been very difficult to observe. The detection of *trans*-**1** would be difficult because its symmetric CO-stretching mode has very low intensity and the antisymmetric CO-stretching mode will overlap with *cis*-**1** mode. In *trans*-**2** the CO-stretching modes shift to lower wave numbers and the symmetric modes of *cis*-**2** and *trans*-**2** overlap. Now, in principle, the antisymmetric stretching mode of *trans*-**2** could be observed but due to the very low concentration of *trans*-**2**, also this would be difficult.

The theoretical dipole moments for *cis*-**1**, *trans*-**1**, *cis*-**2** and *trans*-**2** are 7.20, 0.65, 1.17 and 0.58 D, respectively. The results predict that the *cis* isomers are more stable than the *trans* forms in a polar solvent. In the Monsanto process the solvent is mixture of polar molecules, like water, methanol and acetic acid. To estimate the size of the solvent effect we have performed calculations using the PCM solvation model and methanol as solvent. The total energy difference between *cis*-**1** and *trans*-**1** was 7.52 kcal/mol and between *cis*-**2** and *trans*-**2** 11.87 kcal/mol. From this result we can see that the effect of the solvation does not significantly change the energy differences between *cis* and *trans* forms of the catalysts when compared with the gas phase result.

4. Isomerisation of $[M(CO)_2I_2]^-$ (M = Rh, Ir)

Because the energy differences between the *cis* and *trans* forms of the active catalysts **1** and **2** are not very large, the investigation of the isomerisation from the *cis* to the *trans* geometry is in necessary. Isomerisation processes for the square-planar complexes have been studied widely experimentally and the varieties of the different mechanisms have been proposed in the literature [15].

The simplest transformation from the *cis* to the *trans* structure is an intramolecular ligand exchange process with a tetrahedral like transition state [15]. However, this kind of process is predicted to have a high activation barrier [18] and therefore the exchange mechanism is not commonly accepted.

A preferred route for the isomerisation in the square-planar complexes includes a ligand association step leading to a 5-co-ordinated intermediate complex [15]. After that a consecutive displacement or a pseudorotation follows, both being very fast processes. The consecutive displacement mechanism involves the formation of an ion-pair complex [15]. Ligand dissociation from 5-co-ordinated intermediate concludes the isomerisation. According to the literature [15] the solvent, especially its polarity, is important and affects significantly to the isomerisation mechanism. A polar solvent favours the consecutive

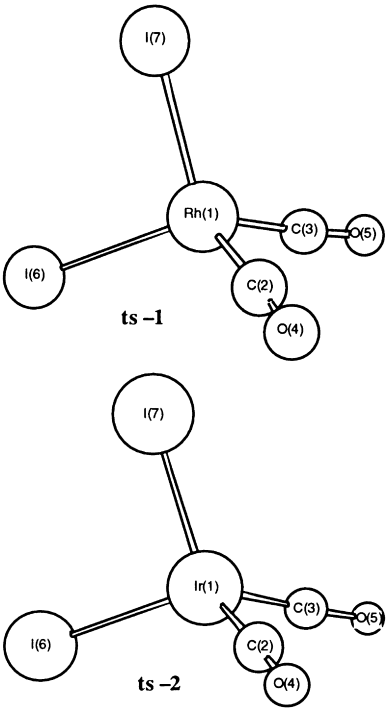

Fig. 3. The singlet state transition states ts-**1** and ts-**2** of the intramolecular ligand exchange process. The calculations result in a tetrahedral like structures.

Table 3
The bond lengths, angles and dihedral angles of the transition states ts-**1** and ts-**2**. M is the metal centre

	ts-**1**	ts-**2**
Distance (Å)		
C(2)–C(3)	2.550	2.565
I(6)–I(7)	4.266	4.141
M(1)–C(2)	1.832	1.837
C(2)–O(4)	1.189	1.194
M(1)–C(3)	1.834	1.837
C(3)–O(5)	1.189	1.194
M(1)–I(6)	2.777	2.795
M(1)–I(7)	2.777	2.795
Angle		
M(1)–C(2)–O(4)	174.7	174.5
M(1)–C(3)–O(5)	174.6	174.5
C(2)–M(1)–I(6)	117.3	118.8
C(2)–M(1)–I(7)	117.2	118.7
C(2)–M(1)–C(3)	88.2	88.5
I(6)–M(1)–I(7)	100.3	95.6
C(3)–M(1)–I(6)	117.6	118.8
C(3)–M(1)–I(7)	117.5	118.7
Dihedral angle		
I(7)–I(6)–M(1)–C(2)	128.1	127.2

displacement whereas a non-polar solvent the pseudorotation.

We started the isomerisation study with the intramolecular ligand exchange process. We have located a singlet transition state complexes for both the catalysts **1** and **2**. The corresponding triplet transition states did not reveal any proper structures. The transition states ts-**1** and ts-**2** of the intramolecular ligand exchange process are illustrated in Fig. 3. Table 3 shows their bond lengths, angles and dihedral angles. The energies of the exchange processes are presented in Fig. 4.

Our results reveal that the singlet transition states have a tetrahedral like geometries (in Fig. 3). The zero-point corrected potential energy barrier for *cis*-**1**–*trans*-**1** isomerisation is 26.13 kcal/mol and the free energy barrier, approximated at 298.15 K, is 25.91 kcal/mol. The corresponding values for the opposite process are 20.48 and 20.96 kcal/mol, respectively. In the case of the catalyst **2** the zero-point corrected potential energy barrier for *cis*-**2**–*trans*-**2**-process is

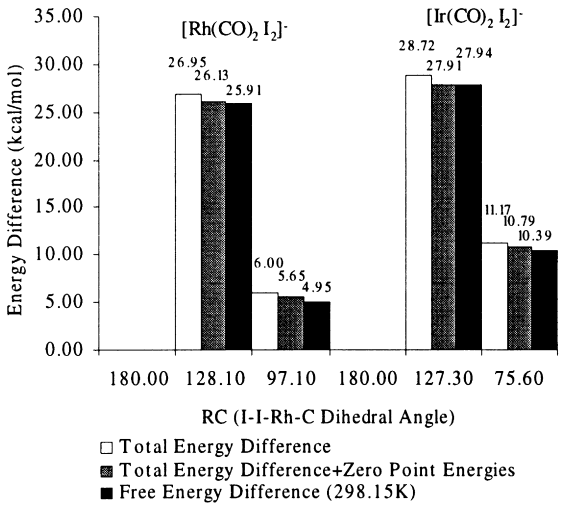

Fig. 4. The energy profiles of the intramolecular ligand exchange process (*cis*-–transition state–*trans*, *cis*-structures on zero level). Figure represents the total energy differences, the zero-point corrected total energy differences and the free energy differences estimated in $T = 298.15$ K. In this case the entropies have no significant effects to the activation energies.

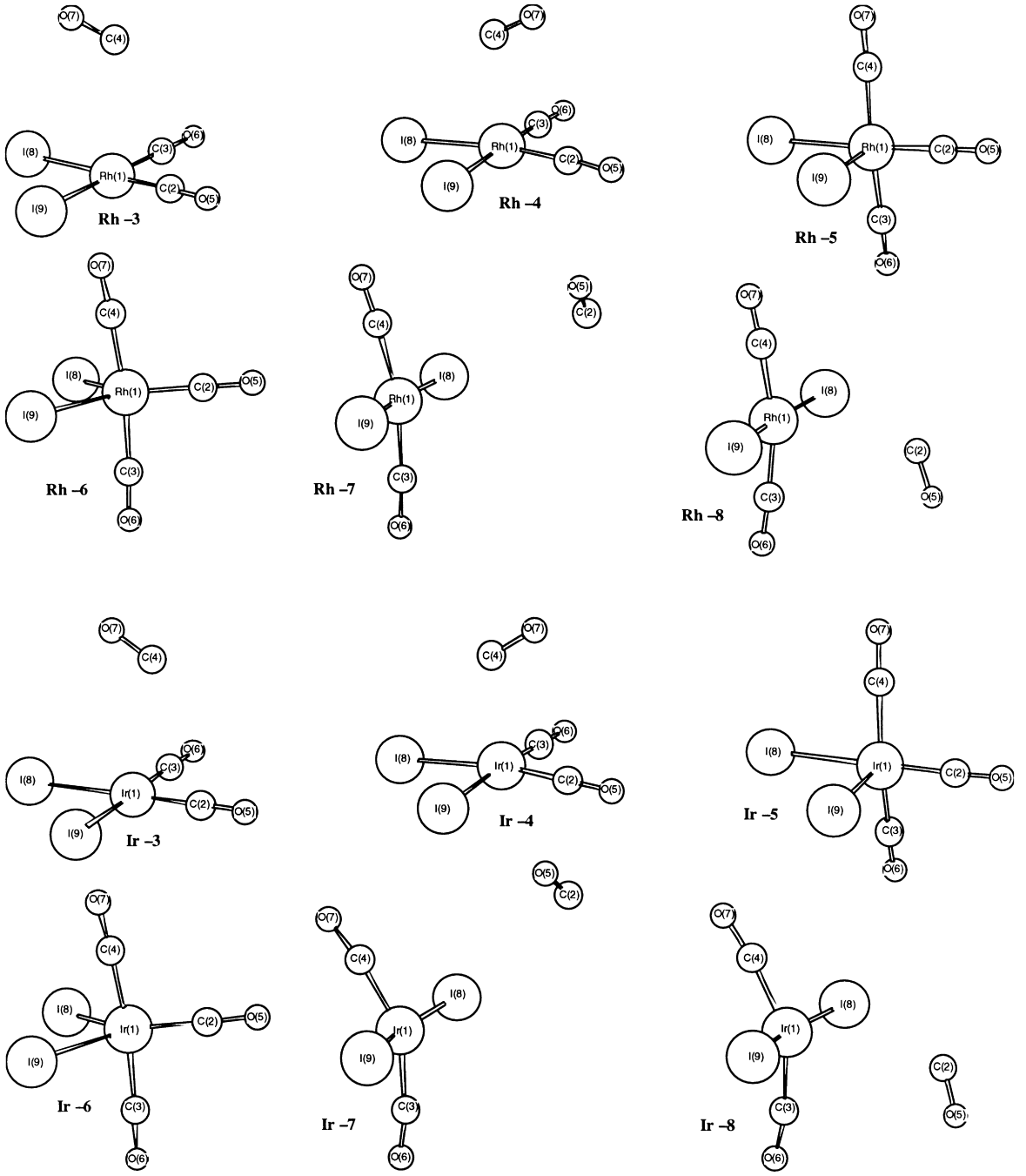

Fig. 5. The stationary points calculated in the isomerisation by the CO-ligand association mechanism. The structures are numbered from Rh-**3** (*cis*-**1** + CO) to Rh-**8** (*trans*-**1** + CO) and from Ir-**3** (*cis*-**2** + CO) to Ir-**8** (*trans*-**2** + CO).

Table 4
The calculated bond lengths and angles of the stationary points in the CO-ligand association mechanism. Rh-**3**–Rh-**8** refer to the structures in Fig. 5

	Rh-**3**	Rh-**4**	Rh-**5**	Rh-**6**	Rh-**7**	Rh-**8**
Distance (Å)						
Rh(1)–C(2)	1.855	1.857	1.871	1.883	5.200	5.993
C(2)–O(5)	1.184	1.183	1.180	1.187	1.168	1.168
Rh(1)–C(3)	1.854	1.858	1.923	1.917	1.906	1.905
C(3)–O(6)	1.184	1.183	1.179	1.175	1.179	1.179
Rh(1)–C(4)	3.448	2.851	1.923	1.917	1.905	1.905
C(4)–O(7)	1.167	1.174	1.179	1.175	1.179	1.179
Rh(1)–I(8)	2.758	2.769	2.792	2.887	2.740	2.739
Rh(1)–I(9)	2.759	2.767	2.992	2.887	2.739	2.739
Angle						
Rh(1)–C(2)–O(5)	178.2	177.3	179.4	180.0	79.1	95.1
Rh(1)–C(3)–O(6)	178.2	178.0	179.5	178.7	175.9	175.9
Rh(1)–C(4)–O(7)	118.8	119.1	179.5	178.7	176.0	175.9
C(2)–Rh(1)–I(8)	179.7	172.8	173.3	128.1	44.0	22.2
C(2)–Rh(1)–I(9)	85.2	84.9	87.3	128.1	130.9	155.3
C(2)–Rh(1)–C(3)	94.9	95.5	93.8	94.7	82.8	71.7
I(8)–Rh(1)–I(9)	94.7	94.8	99.4	103.9	174.7	174.6
C(3)–Rh(1)–I(8)	85.2	84.4	84.8	87.1	90.4	90.6
C(3)–Rh(1)–I(9)	179.7	176.6	102.1	87.1	90.3	90.2

27.91 kcal/mol and the free energy barrier is 27.94 kcal/mol. For the opposite process the corresponding activation parameters are 17.12 and 17.55 kcal/mol. The energy barriers for the intramolecular processes are indeed high in both the *cis–trans* and the *trans–cis* processes. Interestingly, the entropies have very small effects on the energy barriers.

Next we studied the isomerisation using the ligand

Table 5
The calculated bond lengths and angles of the stationary points in the CO-ligand association mechanism. Ir-**3**–Ir-**8** refer to the structures in Fig. 5

	Ir-**3**	Ir-**4**	Ir-**5**	Ir-**6**	Ir-**7**	Ir-**8**
Distance (Å)						
Ir(1)–C(2)	1.855	1.858	1.872	1.872	5.092	5.988
C(2)–O(5)	1.187	1.187	1.183	1.192	1.168	1.168
Ir(1)–C(3)	1.854	1.859	1.923	1.929	1.898	1.897
C(3)–O(6)	1.188	1.189	1.184	1.177	1.187	1.187
Ir(1)–C(4)	3.462	2.743	1.923	1.929	1.898	1.897
C(4)–O(7)	1.168	1.178	1.184	1.177	1.187	1.187
Ir(1)–I(8)	2.777	2.790	2.825	2.911	2.754	2.753
Ir(1)–I(9)	2.777	2.788	2.971	2.911	2.753	2.754
Angle						
Ir(1)–C(2)–O(5)	178.7	177.8	180.0	180.0	77.5	96.6
Ir(1)–C(3)–O(6)	178.7	178.2	177.2	178.0	170.6	170.6
Ir(1)–C(4)–O(7)	111.4	118.9	177.2	178.1	170.6	170.6
C(2)–Ir(1)–I(8)	178.7	173.0	177.4	130.5	46.7	22.6
C(2)–Ir(1)–I(9)	86.4	85.9	87.8	130.5	122.0	151.8
C(2)–Ir(1)–C(3)	94.7	94.9	94.3	94.4	81.3	71.9
I(8)–Ir(1)–I(9)	92.5	92.8	94.8	98.9	167.4	167.4
C(3)–Ir(1)–I(8)	86.4	85.8	84.9	87.2	91.6	91.7
C(3)–Ir(1)–I(9)	178.9	174.9	105.7	87.2	91.5	91.5

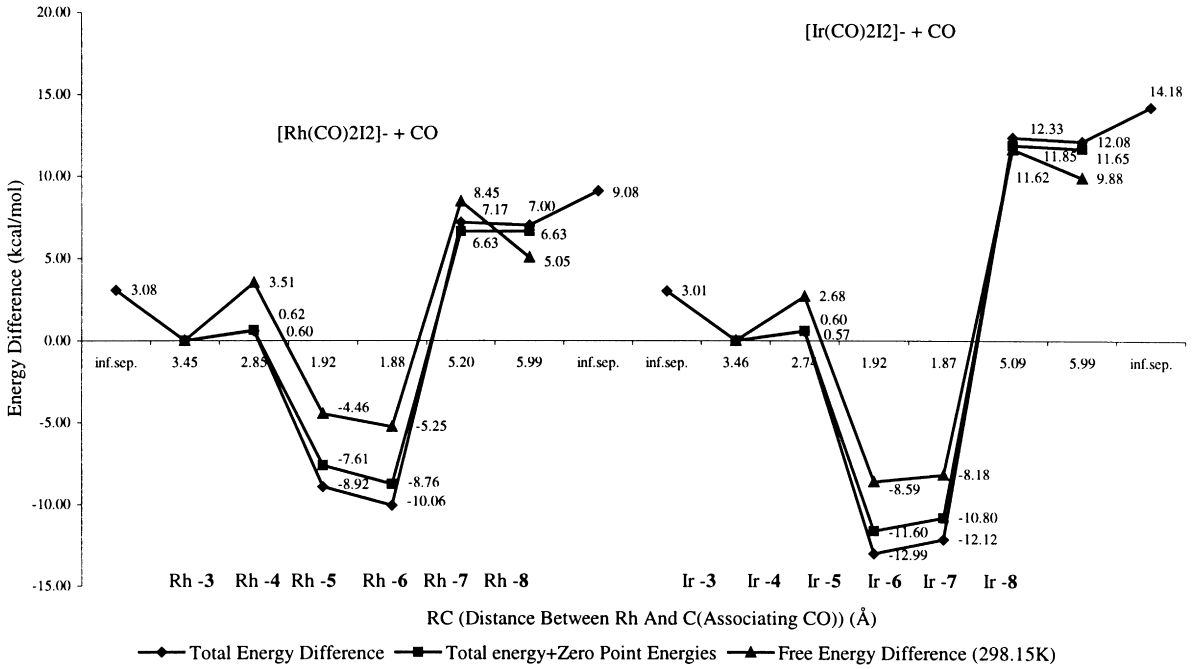

Fig. 6. The energy profiles of the isomerisation by the CO-ligand association mechanism. The figure shows the total energy differences, the zero-point corrected total energy differences and the free energy differences estimated in $T = 298.15$ K. The stationary points refer to the structures Rh-**3**–Rh-**8** and Ir-**3**–Ir-**8**. The total energy of truly separated catalyst and CO is marked with the "inf. sep". The energy differences indicate that in this case the entropy has a significant effect on this process.

association mechanism. Our aim was to locate stationary points on the PES and to evaluate the activation energies to CO association and dissociation from which we hope to get the approximation for the isomerisation barrier. CO-ligand is a natural choice for the association study since CO is one of the initial reactants of the Monsanto and Cativa processes and its concentration is expected to be reasonably high. Because our calculations were performed in the gas phase, we did not try to establish a difference between the consecutive displacement and the pseudorotation, nor did we try to calculate the activation barriers between the 5-co-ordinated intermediates. The calculated stationary points Rh-**3**–Rh-**8** and Ir-**3**–Ir-**8** of the rhodium and iridium systems are illustrated in Fig. 5. The bond lengths and angles of the stationary points are in Table 4 and Table 5. The energy profiles are presented in Fig. 6.

Fig. 5 shows reactant complexes Rh-**3**, Rh-**8**, Ir-**3** and Ir-**8** where CO is at close proximity to the catalysts. We have found these to be in the lower energy than the catalyst and CO at infinite separation. Structural changes between square pyramidal and trigonal bipyramidal geometry in the 5-co-ordinated minimum energy intermediates Rh-**5**–Rh-**6** and Ir-**5**–Ir-**6** make the isomerisation possible. The calculated bond lengths in Tables 4 and 5 show that the associating carbonyl ligand in the 5-co-ordinated species weaken the other Rh–C bonds which implies the reduced back bonding effect. The weakening of the Rh–C bonds may be the key to the energetically easy and fast geometry changes in the 5-co-ordinated intermediates. The minimum energy structures Rh-**5**–Rh-**6** and Ir-**5**–Ir-**6** have never been observed experimentally which indicates that if these structures are present, their lifetime is very short and so on the isomerisation process fast.

The potential energy profiles in Fig. 6 have interesting features. The carbonyl uptakes to Rh-**3**, Rh-**8**, Ir-**3** and Ir-**8** are all very easy in the gas phase. In the *cis*-region the carbonyl association to Rh-**3** and Ir-**3** reveal transition state structures, Rh-**4** and Ir-**4**. Also in the *trans*-sides we have been able to locate transition states Rh-**7** and Ir-**7** with quite long metal

carbonyl distance. Even these structures exist in gas phase it is very unlikely that they are transition states in solution. Interesting is that in the *cis*- and *trans*-sides the reactant complexes and transition states are very different. This is likely due to the difference between the different forms of the active species. The exothermic nature of the carbonyl association is due to forming one new metal–carbonyl bond. The free energy curve in Fig. 6 is also interesting. The entropy effects are more significant in the associative process than in the intramolecular one. Rh-**8** and Ir-**8** are relatively stabilised and the 5-co-ordinated species Rh-**5**–Rh-**6** and Ir-**5**–Ir-**6** are relatively destabilised by the entropy contribution.

The potential energy barrier for the Rh-**3** Rh-**8** isomerisation is 15.39 kcal/mol, including zero-point correction. The free energy barrier at 298.15 K is 13.70 kcal/mol. For the opposite process the zero-point corrected potential energy barrier is 8.23 kcal/mol and the free energy barrier at 298.15 K is 7.97 kcal/mol. For the iridium system the corresponding activation energies are 22.66, 19.80, 12.20 and 11.27 kcal/mol, respectively. In all the cases the carbonyl dissociation from the 5-co-ordinated structures determine the rate of the process as a consequences of easy uptake of the carbonyl ligand.

In addition, we tried to study the isomerisation with iodide as the associating ligand. We have not been able to get any reasonable results because of the instability of the studied systems. Problems with the iodide association are due to the gas phase where the modelling of the iodide is very difficult. Problem could be overcome by including the properly modelled solvent effects. Also a solvent association was tested with methanol as associating ligand. This is expected not to have significance for the isomerisation because it seems that solvent will not associate to active species like CO.

Our studies have so far concentrated on the intramolecular ligand exchange and the associative process. In addition, there are other mechanisms proposed including for example a ligand dissociation mechanism [15]. Because our calculations are performed in the gas phase, the ligand dissociation from a charged square-planar complex could be very difficult to model and therefore these mechanisms at this time are ignored. There is also a recent study concerning the carbonyl exchange reaction [19] that probably could provide a path for isomerisation in $[M(CO)_2I_2]^-$ (M = Rh, Ir). This mechanism will not be discussed in this paper.

5. Results and discussion

We have studied the active catalytic species $[Rh(CO)_2I_2]^-$ (**1**) and $[Ir(CO)_2I_2]^-$ (**2**) and their isomerisation in the gas phase with the density functional-based methods. The *cis* isomers of **1** and **2** have 5.65 and 11.17 kcal/mol lower energy than the *trans* structures. These results are in agreement with the experimental thermodynamics indicating the *cis* complexes to be enthalpy favoured. The entropy effects relatively stabilise the *trans* isomers slightly. The free energy difference between *cis*-**1** and *trans*-**1** is 4.95 kcal/mol and between *cis*-**2** and *trans*-**2** is 10.39 kcal/mol. The *cis* forms of **1** and **2** are almost exactly square planar while the *trans* isomers are twisted. The twisting of the *trans* forms make their symmetric CO-stretching modes IR active, and so both *trans*-**1** and *trans*-**2** could exist in the IR spectra although their detection is difficult due to their low concentrations.

Our isomerisation studies of **1** and **2** include the intramolecular ligand exchange and the associative process. The only transition states found in the intramolecular process are a tetrahedral like structures ts-**1** and ts-**2** with a singlet state. In the intramolecular process calculated activation barriers are high and this isomerisation path is very unlikely. In the associative process we have been able to locate both transition state and minimum energy structures. The results show that the isomerisation in **1** and **2** takes place far easier by the CO-ligand association mechanism than by the intramolecular ligand exchange. For isomerisation by the associative process the free energies of activation are: *cis–trans* 13.70 kcal/mol and *trans–cis* 7.97 kcal/mol, for the rhodium system. For the iridium system the corresponding free energy barriers are 19.80 and 11.27 kcal/mol.

In essence, our results show that the experimentally verified *cis* structures of $[Rh(CO)_2I_2]^-$ (**1**) and $[Ir(CO)_2I_2]^-$ (**2**) are also computationally relatively more stable than the corresponding *trans* forms. However, in the rhodium system the energy difference is small and isomerisation path feasible so previously

unidentified *trans*-**1** is possible. Our preliminary studies [7] have shown that the rate limiting methyl iodide addition to *trans*-**1** takes place more easily than addition to *cis*-**1** and therefore *trans*-**1** can have significance while examining catalytic reactions of the Monsanto process. In the iridium, *cis*-**2** is strongly preferred and involvement of *trans*-**2** to the actual catalysis cycle is not very probable. In more general terms, our results somewhat confirm the experimental view of the square-planar 16-electron d^8-complexes.

Acknowledgements

This work has been financed by Graduate school of computational chemistry and molecular spectroscopy. The authors thank The Finnish Center for Scientific Computing for providing the computational resources needed. TK also thanks Karoliina Honkala and Atte Sillanpää for supportive discussions and language corrections of this paper.

References

[1] P.M. Maitlis, A. Haynes, G.J. Sunley, M.J. Howard, J. Chem. Soc., Dalton Trans. (1996) 2187.
[2] T.R. Griffin, D.B. Cook, A. Haynes, J.M. Pearson, D. Monti, G.E. Morris, J. Am. Chem. Soc. 118 (1996) 3029.
[3] M. Cheong, R. Schmid, T. Ziegler, Organometallics 19 (2000) 1973.
[4] D. Forster, J. Am. Chem. Soc. 98 (1976) 846.
[5] F.E. Paulik, J.F. Roth, Chem. Commun. (1968) 1578.
[6] D. Forster, J. Chem. Soc., Dalton Trans. (1979) 1639.
[7] T. Kinnunen, K. Laasonen, in preparation.
[8] A.D. Becke, J. Chem. Phys. 98 (1993) 5648.
[9] C. Lee, W. Yang, R.G. Parr, Phys. Rev. B 37 (1988) 785.
[10] GAUSSIAN 98 (Revision A.3), M.J. Frisch, G.W. Trucks, H.B. Schlegel, G.E. Scuseria, M.A. Robb, J.R. Cheeseman, V.G. Zakrzewski, J.A. Montgomery, R.E. Stratmann, J.C. Burant, S.Dapprich, J.M. Millam, A.D. Daniels, K.N. Kudin, M.C. Strain, O. Farkas, J. Tomasi, V. Barone, M. Cossi, R. Cammi, B. Mennucci, C. Pomelli, C. Adamo, S. Clifford, J. Ochterski, G.A. Petersson, P.Y. Ayala, Q. Cui, K. Morokuma, D.K. Malick, A.D. Rabuck, K. Raghavachari, J.B. Foresman, J. Cioslowski, J.V. Ortiz, B.B. Stefanov, G. Liu, A. Liashenko, P. Piskorz, I. Komaromi, R. Gomperts, R.L. Martin, D.J. Fox, T. Keith, M.A. Al Laham, C.Y. Peng, A. Nanayakkara, C. Gonzalez, M. Challacombe, P.M.W. Gill, B.G. Johnson, W. Chen, M.W. Wong, J.L. Andres, M. Head-Gordon, E.S. Replogle, J.A. Pople, Gaussian, Inc., Pittsburgh, PA, 1998.
[11] K. Mylvaganam, G.B. Bacskay, N.S. Hush, J. Am. Chem. Soc. 122 (2000) 2041.
[12] K. Mylvaganam, G.B. Bacskay, N.S. Hush, J. Am. Chem. Soc. 121 (1999) 4633.
[13] C.J. Cramer, D.G. Truhlar, Chem. Rev. 99 (1999) 2161.
[14] G.O. Spessard, G.L. Miessler, Organometallic Chemistry, Prentice-Hall, Englewood Cliffs, NJ, 1997.
[15] G.K. Anderson, R.J. Cross, Chem. Soc. Rev. 9 (1980) 185.
[16] A. Haynes, B.E. Mann, G.E. Morris, P.M. Maitlis, J. Am. Chem. Soc. 115 (1993) 4093.
[17] T.W. Dekleva, D. Forster, Adv. Catal. 34 (1986) 81.
[18] T.W. Whitesides, J. Am. Chem. Soc. 91 (1969) 2395.
[19] R. Churland, U. Frey, F. Metz, A.E. Merbach, Inorg. Chem. 39 (2000) 304.